SODIX FOR FULLY AND PARTIALLY COHERENT SOUND SOURCES

Sebastian Oertwig[1], Henri Siller[1], and Stefan Funke[2]

[1]German Aerospace Center (DLR), Institute of Propulsion Technology, Engine Acoustics Department
Müller-Breslau-Str. 8, 10623 Berlin, Germany

[2]Rolls-Royce Deutschland Ltd. & Co KG
Eschenweg 11, OT Dahlewitz, 15827 Blankenfelde-Mahlow, Germany

Abstract

The source localisation method SODIX is capable of determining the amplitudes and the directivity of sound sources based on measurements with a microphone array. The source model of the method has recently been extended with fully coherent sound sources which improves the application of SODIX to tonal noise. This paper presents a further extension of the SODIX source model with partially coherent sources in order to overcome residual effects that cannot be correctly modelled with a fully coherent source model, e.g. due to propagation effects that decorrelate the sound field radiated by a sound source for different receiver positions. The extension relies on a parameterisation of the source directivities and a compressed-sensing based algorithm in combination with an eigenvalue decomposition of the measured cross-spectral matrix to determine the unknown source directivities. The extended localization method with the partially coherent source model is validated using simulated sound sources that have different source directivities and mutual coherence. The results show that only the new source model with partially coherent sound sources is able to resolve the simulated source directivities accurately, when the sources are partially coherent or both coherent and incoherent sources are present.

1 INTRODUCTION

The source localisation method SODIX is capable of determining the amplitudes and the directivity of sound sources based on measurements with a microphone array. SODIX stands for *SOurce DIrectivity modelling in the cross-spectral matriX* and is mainly being developed for the analysis of broadband noise sources in static engine noise testing [1–3]. The SODIX method is able to quantify the contribution of individual source regions as e.g. the intake, the nozzle, and the jet to the overall radiated noise.

Figure 1 shows a typical measurement setup at an outdoor engine noise test facility with a linear microphone array placed on the testbed ground in parallel with the engine axis. The linear microphone array is densely populated with approximately 250 microphones and provides a polar resolution of approximately $0.6°$.
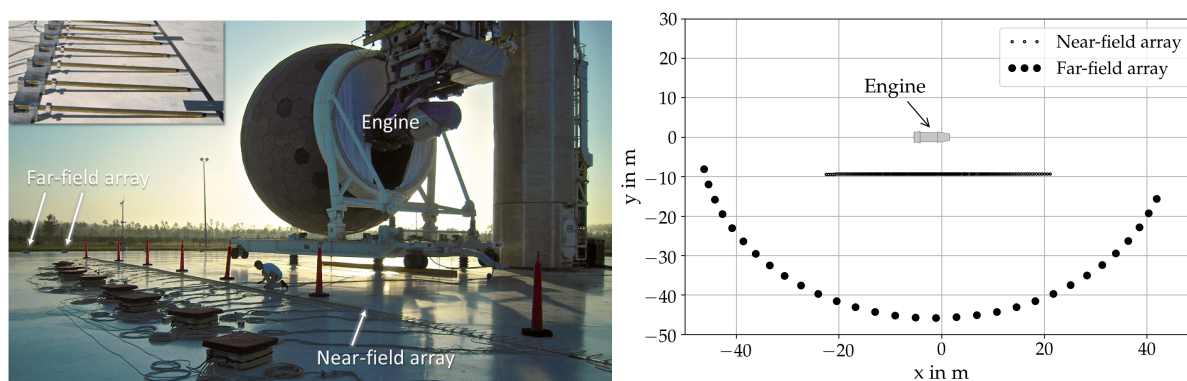
(a) Typical measurement setup (taken from [3])   *(b) Microphone array positions*

Figure 1: Measurement setup with microphone arrays at a static engine noise test facility.

Compared to other source localisation methods, SODIX has the unique feature that it is able to determine both the amplitude and the directivity of sound sources. For outdoor engine noise tests, SODIX has been applied to data from a large microphone array in the near-field of an engine as well as to data from a sparse array in the far-field [3, 4]. Also, the application of SODIX to microphone measurements in reverberant test-cells for turbofan engines has been studied [5].

The SODIX method was originally developed for the analysis of broadband noise sources and initially used an incoherent point source model with real-valued source amplitudes. An updated version of the incoherent source model that includes the modelling of the phase of the sources as well as an extension to analyse fully coherent sound sources have been recently presented [6]. The coherent source model improves the application of the localisation method to tonal noise sources in static engine noise testing like e.g. fan tones that radiate from both the intake and the nozzle exit. A cyclo-stationary analysis has been performed in the pre-processing of the microphone array data in order to meet the assumption of fully coherent sound sources. This analysis technique separates the part of the spectra that is coherent with the shaft rotation of the engine from fluctuating components at the same frequencies. The rotor-coherent part of the fan tones results from source mechanisms that correlate with the rotation of the engine shaft, e.g. the interaction of the rotor wakes with the stator vanes of the fan stage. The contribution of the tone that is not coherent with the rotor can be either associated with other source mechanisms that do not correlate with the rotation of the engine shaft like the interaction of turbulent flow with the fan, or it can result from propagation effects that decorrelate the sound field radiated by a sound source for different receiver positions, e.g. when sound propagates through turbulent flow.

So far, the fluctuating component of the spectra has been discarded and only the coherent part of the microphone spectra has been analysed. It has been shown that the extended SODIX method for fully coherent sound sources is able to localize a fan tone radiating from the engine

intake and the nozzle at the expected positions [6]. The derived source directivities were also reasonable, but have shown unrealistic over-predictions at both ends of the microphone array where the spatial resolution of the microphone array is lower.

This papers presents a further extension of the source localisation method SODIX for partially coherent sound sources that overcomes the assumption of fully coherent sound sources. This is particularly important when propagation effects decorrelate the sound field of the sources or coherent and incoherent sound sources are present at the same frequency. The paper shows a thorough description of the analysis technique that is based on the extension of the source model used in SODIX, a parameterisation of the source directivities using base functions, and the use of a compressed-sensing based algorithm in combination with an eigenvalue decomposition of the measured cross-spectral matrix to determine the unknown source directivities. Finally, the extended SODIX method is validated using simulated sound sources that exhibit different mutual coherence and different source directivities. The source localisation results derived with the new SODIX method with the partially coherent source model are compared to those from the previous version with the incoherent source model in order to underline the improvements of the localization results with the new, extended SODIX method.

2 METHODOLOGY

The source localisation method SODIX is capable of determining the amplitudes as well as the directivity of sound sources. The method was originally developed for broadband noise sources only [1–3, 7] as an extension of the Spectral Estimation Method (SEM) [8, 9]. This section gives a thorough description of the SODIX method, beginning with the incoherent source model as a reference. Then, the extended source model for coherent sound sources is presented. Finally, an approach for resolving partially coherent sound sources using a compressed-sensing based algorithm in combination with an eigenvalue decomposition of the measured cross-spectral matrix as proposed by *Behn et al.* [10] is outlined.

2.1 Incoherent source model

The SODIX model of the cross-spectral matrix consists of *incoherent* point sources **D** with individual amplitudes from all sources $j = 1, \ldots, J$ to all microphones $m = 1, \ldots, M$. The microphone cross-spectra are therefore modelled by the incoherent superposition of the directive sources:

$$C_{mn}^{\mathrm{mod}} = \sum_{j=1}^{J} g_{jm} D_{jm} D_{jn}^* g_{jn}^* \,, \tag{1}$$

where g are the steering vectors that describe the known sound propagation from the sources to the microphones. The main assumption of the SODIX source model in equation (1) is that the sources are mutually *incoherent* which is mathematically described by vanishing cross-powers for sources at different locations j and k:

$$\overline{D_{jm}D_{kn}^*} = \begin{cases} D_{jm}D_{kn}^* \,, & \text{if } j = k \,, \\ 0 \,, & \text{if } j \neq k \,. \end{cases} \tag{2}$$

For the incoherent source model, the source directivities $\mathbf{D}$ are determined by a least-squares fit between the measured and the modelled cross-spectral matrix which is solved iteratively using a conjugate gradient method [5]:

$$F(\mathbf{D}) = \left\| \mathbf{C} - \mathbf{C}^{\mathrm{mod}} \right\|^2 + \sigma R(\mathbf{D}) . \tag{3}$$

The cost function in equation (3) includes an additional regularization term R that helps to find stable solutions, even when the number of unknown source amplitudes is much higher than the known entries in the measured cross-spectral matrix.

2.2 Coherent source model

In the presence of coherent sound sources, the cross-powers of sources at different locations have to be included in the source model. This implies that equation (2) is substituted for all sources by:

$$\overline{D_{jm}D_{kn}^*} = D_{jm}D_{kn}^* , \tag{4}$$

which now includes the off-diagonal elements of the source cross-spectral matrix. Therefore, additional terms appear in the coherent SODIX model of the measured cross-spectral matrix that now becomes:

$$C_{mn}^{\mathrm{mod}} = \sum_{j=1}^{J} \sum_{k=1}^{J} g_{jm} D_{jm} D_{kn}^* g_{kn}^* . \tag{5}$$

Note the second sum over source indices k in comparison to the incoherent source model in equation (1). The full model of the cross-spectral matrix $\mathbf{C}^{\mathrm{mod}}$ can then be written as follows:

$$\begin{aligned} \mathbf{C}^{\mathrm{mod}} &= \hat{\mathbf{G}}\hat{\mathbf{D}}\hat{\mathbf{D}}^H\hat{\mathbf{G}}^H \\ &= \hat{\mathbf{G}}\mathbf{S_{dd}}\hat{\mathbf{G}}^H , \end{aligned} \tag{6}$$

where $\hat{\mathbf{G}}$ is the system matrix, $\hat{\mathbf{D}}$ is the solution vector containing the source directivities, and $\mathbf{S_{dd}} = \hat{\mathbf{D}}\hat{\mathbf{D}}^H$ is the full source cross-spectral matrix. The system matrix $\hat{\mathbf{G}}$ consists of diagonal matrices with the sound propagation functions g_{jm} as elements:

$$\hat{\mathbf{G}} = \begin{bmatrix} g_{11} & 0 & \dots & 0 & \dots & g_{J1} & 0 & \dots & 0 \\ 0 & g_{12} & \dots & 0 & \dots & 0 & g_{J2} & \dots & 0 \\ \vdots & \vdots & \ddots & \vdots & \dots & \vdots & \vdots & \ddots & \vdots \\ 0 & 0 & \dots & g_{1M} & \dots & 0 & 0 & \dots & g_{JM} \end{bmatrix} \in \mathbb{C}^{M \times MJ} . \tag{7}$$

The solution vector $\hat{\mathbf{D}}$ is composed of the individual source directivities D_{jm} arranged in blocks $\mathbf{d}_j$ for each single source j:

$$\hat{\mathbf{D}} = \left[\mathbf{d}_1, \mathbf{d}_2, \dots, \mathbf{d}_J \right]^T = [D_{11} \dots D_{1M} \, D_{21} \dots D_{2M} \dots D_{J1} \dots D_{JM}]^T \in \mathbb{C}^{MJ} . \tag{8}$$

2.3 Resolving partially coherent sound sources

In technical applications, sound sources are neither completely incoherent nor fully coherent. Therefore, this paper presents an extension of the source localisation method SODIX that aims to resolve partially coherent sound sources and their directivities. The analysis technique is based on an eigenvalue decomposition of the measured cross-spectral matrix and a compressed-sensing based algorithm proposed by *Behn et al.* [10] for the analysis of turbo-machinery induct modes. The aim of compressed-sensing is to find a solution with the smallest number of elements which allows to reconstruct sparse signals. This is a good approach for the analysis of the sound radiation of tonal noise from turbofan engines as engine tones radiate from distinct locations like the engine intake, the bypass, and the nozzle exit. A compressed-sensing based algorithm has already been used for solving the fully coherent source model within SODIX [6]. The first step of the new analysis technique is to perform the eigenvalue decomposition of the measured cross-spectral matrix:

$$\mathbf{C} = \mathbf{U}\mathbf{\Lambda}\mathbf{U}^H , \tag{9}$$

where $\mathbf{U}$ is a unitary matrix with the eigenvectors $\mathbf{u}_i$ as columns and $\mathbf{\Lambda}$ is a diagonal matrix with the eigenvalues λ_i on the main diagonal. For the further analysis, the eigenvectors are normalised with the corresponding eigenvalues:

$$\mathbf{v}_i = \sqrt{\lambda_i}\mathbf{u}_i . \tag{10}$$

The main difference to the previous analysis for the fully coherent source model is that the compressed-sensing algorithm BOMP (block orthogonal matching pursuit) is now used individually for each eigenvalue of the measured cross-spectral matrix:

$$\underset{\mathbf{d}_{\mathbf{j}_i}\in\mathbb{C}^M}{\arg\min} \left\|\mathbf{d}_{\mathbf{j}_i}\right\|_1 , \quad \text{subject to} \quad \left\|\mathbf{v}_i - \hat{\mathbf{G}}\hat{\mathbf{D}}_i\right\|_2 \leq \varepsilon , \tag{11}$$

where $\mathbf{d}_{\mathbf{j}}$ is the source directivity of the source j arranged in a block according to equation (8), $\mathbf{d}_{\mathbf{j}_i}$ is the contribution of the i-th eigenvalue to that source directivity $\mathbf{d}_{\mathbf{j}}$, $\hat{\mathbf{D}}_i$ contains the full source directivities for all sources that correspond to the i-th eigenvalue, and ε is an error bound, e.g. the measurement noise energy. The full source cross-spectra are then obtained by a superposition of the source spectra for all eigenvalues which allows to determine partially coherent sources with individual directivity:

$$\mathbf{S_{dd}} = \sum_{i=1}^{M} \hat{\mathbf{D}}_i\hat{\mathbf{D}}_i^H . \tag{12}$$

2.4 Parameterisation of the source directivity with base functions

The dimension of the system matrix $\hat{\mathbf{G}} \in \mathbb{C}^{M\times MJ}$ shows that the equation system (6) is underdetermined. Therefore, base functions are introduced in order to reduce the degrees of freedom of the solution vector. The directivity of a single source is then expressed as a weighted sum of

L elements of a set of base functions B that are evaluated at a specific coordinate φ_{jm}:

$$D_{jm} = D_{j,\mathbf{x}_j}\left(\varphi_{jm}\right) = \sum_{l=1}^{L} x_{jl} B_l\left(\varphi_{jm}\right) \ . \tag{13}$$

In equation (13), x is a weighting factor for the individual elements of the set of base functions and becomes the new variable to be solved for. The parameterisation of the source directivities can be formulated as a linear system of equations for the new solution vector $\mathbf{x}_j$:

$$\mathbf{d_j} = \begin{bmatrix} D_{j1} \\ \vdots \\ D_{jM} \end{bmatrix} = \mathbf{B_j x_j} = \begin{bmatrix} B_1(\varphi_{j1}) & B_2(\varphi_{j1}) & \dots & B_L(\varphi_{j1}) \\ \vdots & \vdots & \ddots & \vdots \\ B_1(\varphi_{jM}) & B_2(\varphi_{jM}) & \dots & B_L(\varphi_{jM}) \end{bmatrix} \begin{bmatrix} x_{j1} \\ \vdots \\ x_{jL} \end{bmatrix} \ . \tag{14}$$

It should be noted here that equation (14) only describes the parameterised source directivity of a single source j. The fully parameterised solution vector is given by inserting equation (14) into equation (8) which then connects the source directivities and the new weighting factors with the block-diagonal matrix $\hat{\mathbf{B}}$ that contains the base functions:

$$\hat{\mathbf{D}} = \begin{bmatrix} \mathbf{d_1} \\ \vdots \\ \mathbf{d}_J \end{bmatrix} = \hat{\mathbf{B}}\hat{\mathbf{x}} = \begin{bmatrix} \mathbf{B_1} & & \mathbf{0} \\ & \ddots & \\ \mathbf{0} & & \mathbf{B_J} \end{bmatrix} \begin{bmatrix} \mathbf{x_1} \\ \vdots \\ \mathbf{x_J} \end{bmatrix} \ . \tag{15}$$

The original problem for the unknown source directivities $\mathbf{D}$ in equation (6) can now be expressed for the weights $\mathbf{x}$ of the used set of base functions:

$$\mathbf{C}^{\mathrm{mod}} = \mathbf{PP}^H \quad \text{with} \quad \mathbf{P} = \hat{\mathbf{G}}\hat{\mathbf{D}} = \hat{\mathbf{G}}\hat{\mathbf{B}}\hat{\mathbf{x}} = \mathbf{\Psi}\hat{\mathbf{x}} \ . \tag{16}$$

In the case of fully coherent sound sources with a magnitude-squared coherence $\gamma^2 = 1$, it is sufficient to model the complex pressure vector $\mathbf{p} = [p_1, \dots, p_m]^T$ rather than the full cross-spectral matrix because then the cross-spectral matrix is easily expressed as an outer product of the complex pressure vector $\mathbf{C} = \mathbf{pp}^H$.

2.5 Definition of base functions

A preliminary study on the selection of the base functions has been carried out in [11]. Three different sets of base functions have been proposed: Bernstein polynomials, piecewise linear base functions, and harmonic base functions. Here, only the Bernstein polynomials and the harmonic base functions are presented because the linear base functions perform similar to the harmonic base functions. Equations (17) and (18) provide the mathematical definitions of the two different sets of base functions.

Bernstein polynomials

Bernstein polynomials are closely related to spline functions and can be written as:

$$B_i(t) = \binom{n}{i} t^i (1-t)^{n-i} \quad \text{with} \quad i = 0, \ldots, n . \tag{17}$$

Here, the index becomes $i = l - 1$ with $l = 1, \ldots, L$ and L being the number of used base elements.

Harmonic base functions

The harmonic base functions of the order d with $L = 2d + 1$ elements are given by:

$$B_l(t) = e^{i(l-d-1)2\pi t} \quad \text{with} \quad l = 1, \ldots, L . \tag{18}$$

Figure 2 compares the two sets of base functions for the same number of base curves on a normalised interval, e.g. an axial coordinate for a linear microphone array or a polar angle in the far-field normalised with respect to the bounds.
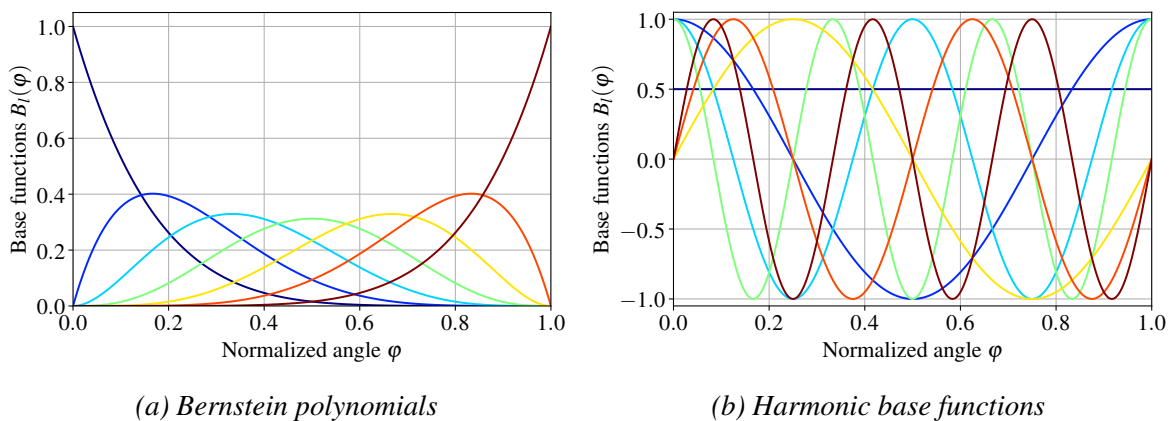

(a) Bernstein polynomials   *(b) Harmonic base functions*

Figure 2: Different sets of base functions used for the parameterisation of the source directivities.

The preliminary study in [11] has indicated that Bernstein polynomials perform better than piecewise linear and harmonic base functions for simulated sound sources with relatively smooth directivities. However, a first application to a fan tone measured during static engine noise testing has shown that the parameterisation with Bernstein polynomials can lead to very large over-predictions of the source directivities towards the outer ends of the linear microphone array [6]. This effect was partially reduced by omitting a few microphones at both ends of the array from the analysis that provide a poor spatial resolution.

3 VALIDATION WITH SIMULATED SOUND SOURCES

This section presents the source localisation results of the extended SODIX method with the partially coherent source model for simulated sound sources. Three testcases that feature different source directivities and different mutual coherence of the simulated sound sources have been created using the open-source software *Acoular* [12]. First, the extended SODIX method is applied to simulated monopole sources that are either mutually incoherent or fully coherent. Then, the method is applied to another simulation that features different directive sound sources that are again either mutually incoherent or fully coherent. Finally, the extended SODIX method is applied to a third simulation that features directive sound sources that are now partially coherent.

3.1 Monopole sound sources with different mutual coherence

A simulation of monopole sound sources with different mutual coherence was performed to study the localisation results for the different source models used in SODIX. The simulated sound sources are aligned on an axis that is parallel with a microphone array with approximately 250 microphones that is similar to an array used for source localisation in static engine noise testing. Two coherent monopole sources with a magnitude-squared coherence $\gamma^2 = 1$ and the same amplitude are located at $x = -5\,\text{m}$ and $x = 0\,\text{m}$. An additional incoherent monopole source with half the amplitude of the other sources is located at $x = 2\,\text{m}$.

Figure 3 shows the source localisation results derived with SODIX using different source models. On the left-hand side, typical source maps are presented that show the source amplitudes with the source position on the horizontal axis and the emission angle on the vertical axis. The positions of the simulated sources are indicated by the grey, dashed lines. The right-hand side of figure 3 shows a quantitative comparison of the source directivities that have been extracted from the source maps for individual source areas around the simulated source positions with the simulated sound pressure levels indicated by the dashed lines.

All three source models can reproduce the sound pressure levels at the microphones (black dashed and solid curves) accurately, however the results for the individual sources (coloured lines) can show large deviations from the simulated levels depending on which source model is used for the calculations.

The localisation results derived with the incoherent source model are presented in figure 3a as a reference in order to emphasize the improvements of the localisation results with the new, extended SODIX method. It should be noted here, that an improved version of the incoherent source model has been used that includes the modelling of the phase of the sources as presented in [6]. All three sources are localized at the correct position. However, the uniform directivity of the two coherent monopoles is not well determined with the incoherent source model. The mutual coherence of the two sound sources leads to distinct lobes and phase jumps along the microphone array which cannot be accurately modelled by an incoherent superposition of sources. The overall source directivity of the third incoherent source is better reproduced than those of the two coherent monopoles, although the derived source levels are lower than the simulated source amplitude over the whole angular range.

(a) Incoherent source model

(b) Fully coherent source model
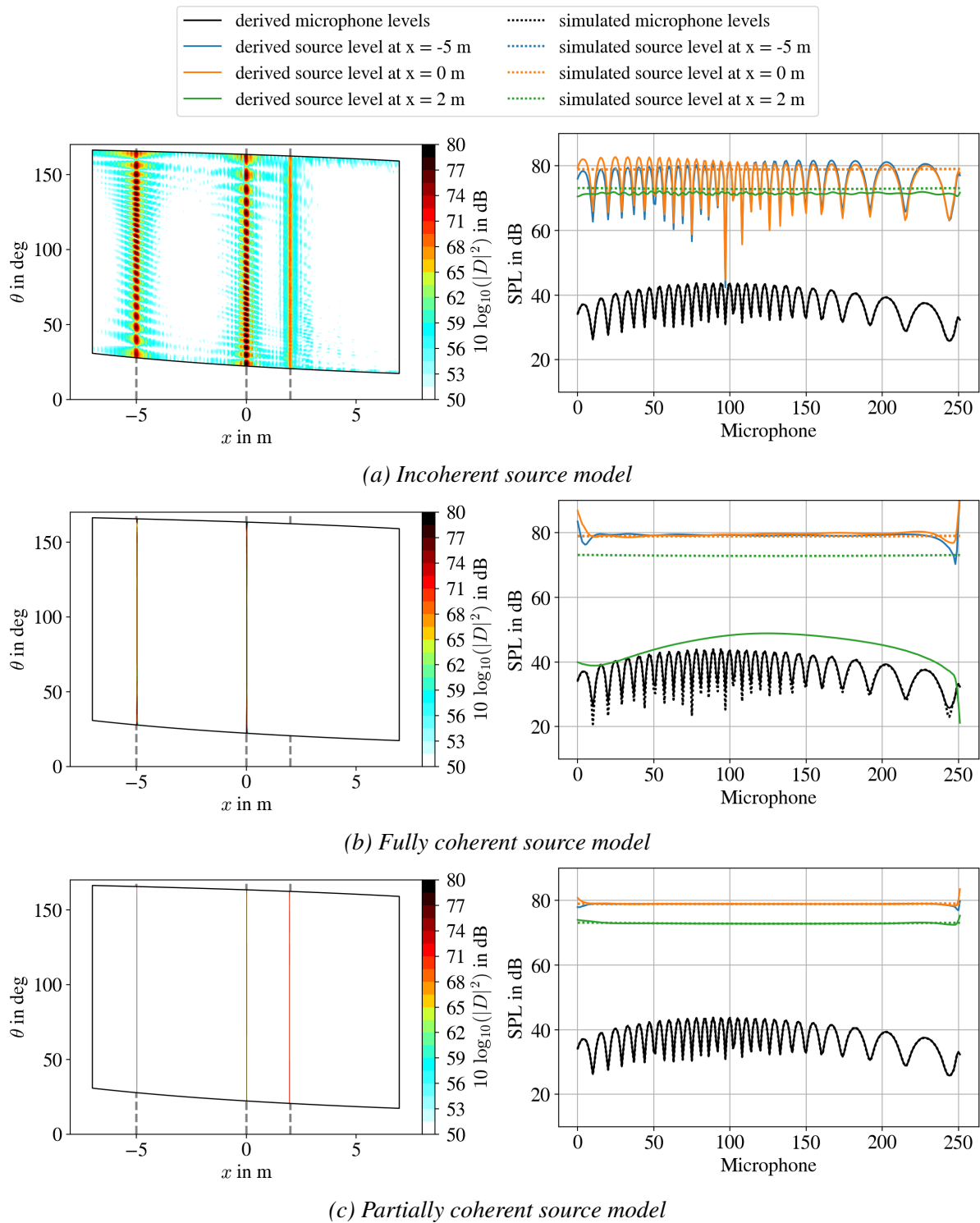

(c) Partially coherent source model

Figure 3: Source localisation results derived with SODIX for a simulation of two fully coherent monopoles and an additional incoherent monopole source. The maps show the source directivities determined with SODIX using a source model with incoherent sources (top), fully coherent sources (center), and partially coherent sources (bottom). The sources at $x = -5$ m and $x = 0$ m have a simulated level of 78.9 dB and the source at $x = 2$ m has a a simulated level of 72.9 dB as indicated by the dashed lines.

The extension to a fully coherent source model improves the source localisation for the two coherent monopole sources, as shown in figure 3b. The source directivities of the two coherent monopoles are relatively uniform except for the extreme positions at the far ends of the array, where the source directivities fluctuate with strong amplitude variations. Such a phenomenon has already been observed for the application of the fully coherent source model to measured engine noise data and might result from a low spatial resolution of the microphones at both ends of the array [6]. The third incoherent sound source is determined with a lower amplitude when a fully coherent source model is used. The failure to correctly detect this sound source might also explain the slight over-prediction of the two coherent monopoles with this source model.

The extension of the SODIX source model with partially coherent sound sources further improves the source localisation results as shown in figure 3c. The two coherent monopoles and the additional incoherent monopole source are now accurately detected with their simulated source directivities. There are still some artefacts towards both ends of the microphone array, but the deviations from the simulated levels are much smaller than for the fully coherent source model.

3.2 Directive sound sources with different mutual coherence

A second simulation with directive sound sources has been performed to further investigate the localisation results for the different source models used in SODIX. This simulation features two sources at $x = -5$ m and $x = 0$ m that have a directivity similar to a stationary dipole and are mutually coherent with a magnitude-squared coherence $\gamma^2 = 1$. The third source at $x = 2$ m has a continuous directivity with a peak radiation around $90°$ and is incoherent with the two dipole sound sources. The source localisation results for this simulation are presented in figure 4.

Similar to the previous simulation, all three source models can reproduce the sound pressure levels at the microphones (black dashed and solid curves), although the results for the individual sources (coloured lines) can show large deviations from the simulated source levels depending on the used source model.

Figure 4a presents the source localisation results for the incoherent source model as a reference. Similar to the simulation with monopoles, the source model with incoherent sound sources is not able to determine the true directivity of the coherent sound sources. Again, the third incoherent sound source is reproduced better than the two coherent dipole sources, but its amplitude is lower than the simulated amplitude.

The extension to fully coherent sound sources in figure 4b helps to improve the localisation of the coherent dipole sources, although the source amplitudes are over-predicted. This phenomenon might be the result of a compensation of the third incoherent sound source that is not well determined with the fully coherent source model.

The extension of the SODIX source model with partially coherent sound sources further improves the source localisation results as shown in figure 4c. The two coherent dipoles and the third incoherent directive source are now accurately detected at the correct position and with their directivity within the presented dynamic range of 60 dB. There are still some minor artifacts in terms of oscillations towards both ends of the microphone array, but these artifacts are drastically reduced in comparison to the fully coherent source model. In general, the source localisation results for this simulation confirm the observation from the first simulation with monopole sources that the source model with partially coherent sound sources performs much better in a sound field with both coherent and incoherent sound sources.

(a) Incoherent source model

(b) Fully coherent source model
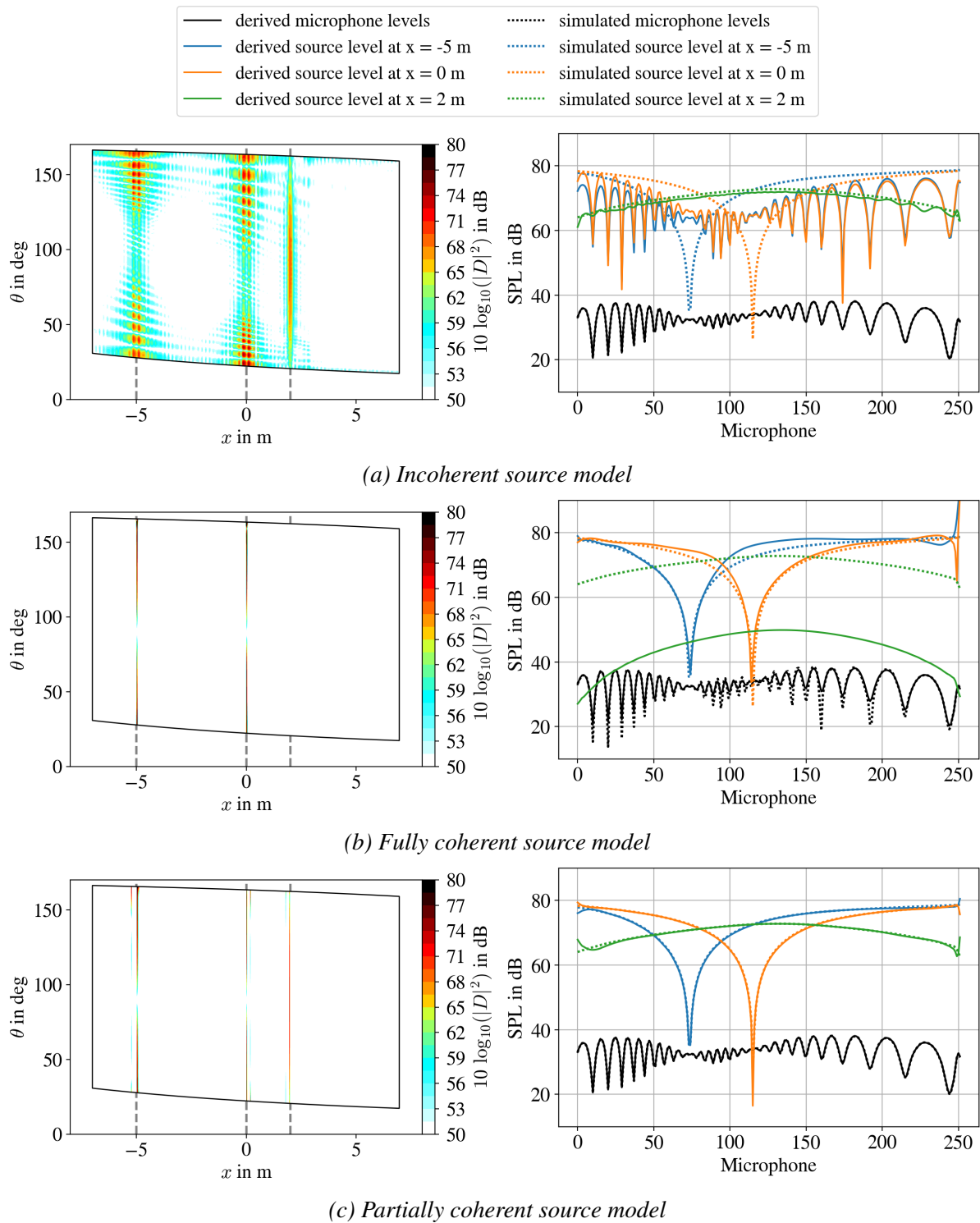

(c) Partially coherent source model

Figure 4: Source localisation results derived with SODIX for a simulation of two fully coherent dipoles and an additional incoherent directive source. The maps show the source directivities determined with SODIX using a source model with incoherent sources (top), fully coherent sources (center), and partially coherent sources (bottom). The simulated levels are indicated by the dashed lines.

3.3 Directive sound sources with partial coherence

The previous simulation with directive sound sources has been modified to feature partially coherent sound sources in order to further investigate the localisation results for the different source models used in SODIX. This simulation has two sources at $x = -5\,\mathrm{m}$ and $x = 0\,\mathrm{m}$ that have a directivity similar to a stationary dipole and are now partially coherent with a magnitude-squared coherence $\gamma^2 \approx 0.25$. The third source at $x = 2\,\mathrm{m}$ has a continuous directivity with a peak radiation around $90°$ and is incoherent with the two other sound sources. The source localisation results for this simulation are presented in figure 5.

Similar to the previous simulations, all three source models can reproduce the sound pressure levels at the microphones (black dashed and solid curves), although the results for the individual sources (coloured lines) can show large deviations from the simulated source levels depending on the used source model.

Figure 5a presents the source localisation results for the incoherent source model as a reference. Similar to the previous simulations with either fully coherent or incoherent sound sources, the SODIX source model with incoherent sound sources is not able to resolve the true directivity of the simulated, partially coherent sound sources. The derived source directivities of the two partially coherent dipole sources show large oscillations that do not match the simulated sound pressure levels. However, this phenomenon is much weaker than for the previous simulation with fully coherent sound sources due to the reduced source coherence of $\gamma^2 \approx 0.25$. The third incoherent sound source is again better reproduced than the two partially coherent dipole sources, but its amplitude is lower than the simulated amplitude.

The extension to fully coherent sound sources in figure 5b helps to improve the localisation of the partially coherent dipole sources, although the derived amplitudes partly deviate from the simulated sound pressure levels. This phenomenon might result from the fact that the fully coherent source model can only determine the coherent part of the sound field and therefore omits the incoherent part of the simulated source amplitude.

The extension of the SODIX source model with partially coherent sound sources further improves the source localisation results as shown in figure 5c. The two partially coherent dipoles and the third incoherent directive source are now accurately detected at the correct position and with their directivity within the presented dynamic range of $60\,\mathrm{dB}$. There are still some minor artifacts in terms of oscillations towards both ends of the microphone array, but these artifacts are drastically reduced in comparison to the fully coherent source model. However, the appearance and the strength of the spurious artifacts also depend on other parameters like the microphone layout, the number of base functions, or the radiation pattern of the sources.

In general, the localisation results for this third simulation show that only the new, extended SODIX method with partially coherent sound sources can reproduce the simulated directivities when partially coherent sound sources are present.

(a) Incoherent source model

(b) Fully coherent source model
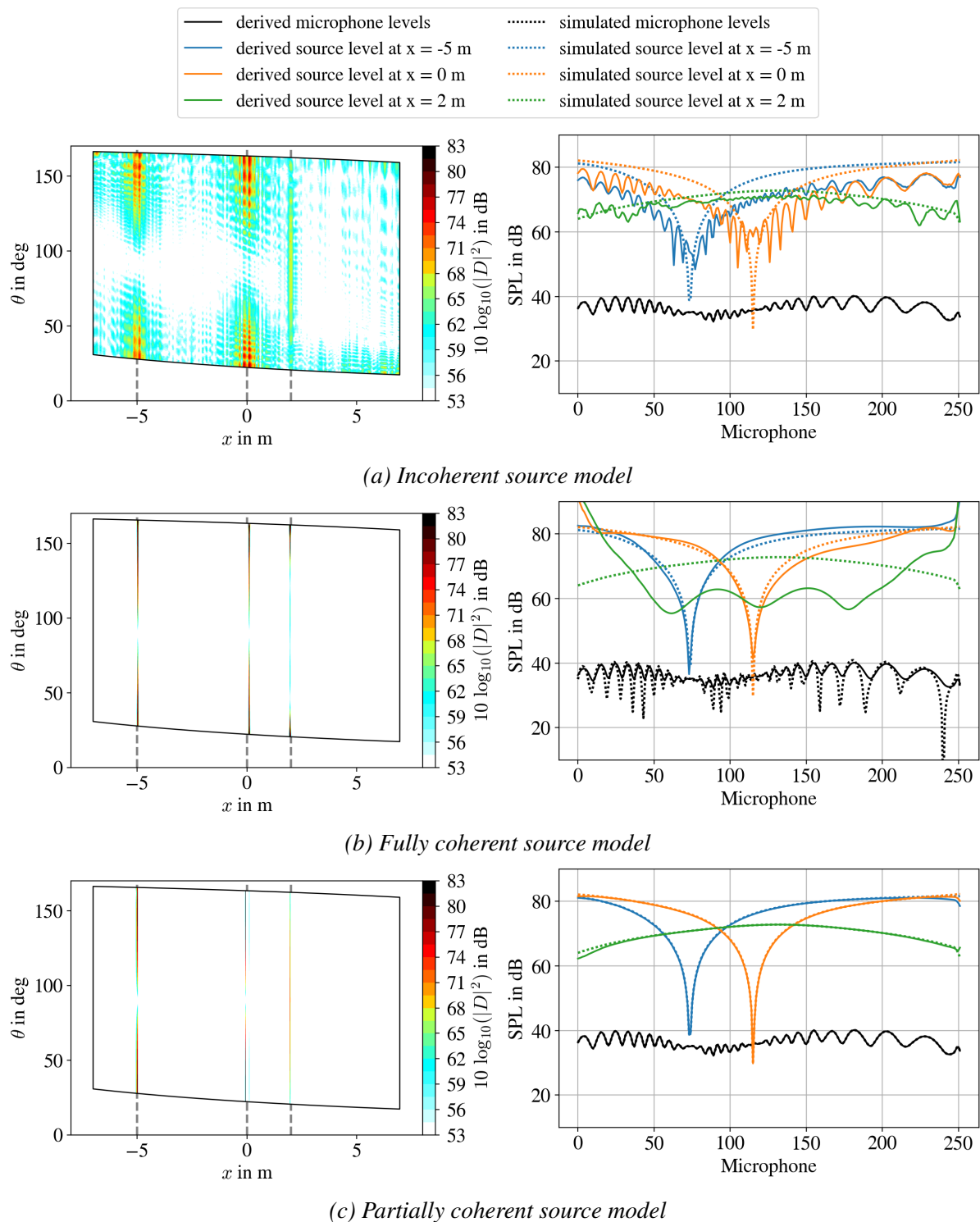

(c) Partially coherent source model

Figure 5: Source localisation results derived with SODIX for a simulation of two partially coherent dipoles and an additional incoherent directive source. The maps show the source directivities determined with SODIX using a source model with incoherent sources (top), fully coherent sources (center), and partially coherent sources (bottom). The simulated levels are indicated by the dashed lines.

4 CONCLUSIONS

The source localisation method SODIX has been extended for the analysis of coherent sound sources. This paper presents a further extension of the method with partially coherent sound sources that overcomes the assumption of fully coherent sound sources. This is particularly important when propagation effects decorrelate the sound field of the sources or coherent and incoherent sound sources are present at the same frequency.

The extension of the method is based on a coherent source model, a parameterisation of the source directivities with base functions, and a compressed-sensing based algorithm in combination with an eigenvalue decomposition of the measured cross-spectral matrix.

The new, extended SODIX method with partially coherent sound sources has been validated using simulated sound sources with different directivities and different mutual coherence. The localisation results have shown that the initial incoherent source model cannot be applied when partially or fully coherent sound sources are present. The fully coherent source model improves the localisation results for fully coherent sound sources, but fails to resolve incoherent and partially coherent sound sources. The extension of the source model with partially coherent sound sources further improves the determination of fully coherent, partially coherent, and incoherent sound sources at the same frequency. Also, the partially coherent source model determines both the coherent and incoherent sound sources in one calculation.

ACKNOWLEDGEMENTS

REFERENCES

[1] U. Michel and S. Funke. Noise Source Analysis of an Aeroengine with a New Inverse Method SODIX. In *14th AIAA/CEAS Aeroacoustics Conference (29th AIAA Aeroacoustics Conference), May 5-7, 2008, Vancouver, British Columbia*, number AIAA 2008-2860, 2008.

[2] S. Funke, A. Skorpel, and U. Michel. An extended formulation of the SODIX method with application to aeroengine broadband noise. In *18th AIAA/CEAS Aeroacoustics Conference, 4-6 June 2012, Colorado Springs, USA*, number AIAA 2012-2276, 2012.

[3] Stefan Funke. *Ein Mikrofonarray-Verfahren zur Untersuchung der Schallabstrahlung von Turbofantriebwerken*. Doctoral thesis, Technische Universität Berlin, Berlin, 2017.

[4] Sebastian Oertwig, Stefan Funke, and Henri Siller. Improving source localisation with SODIX for a sparse microphone array. In *7th Berlin Beamforming Conference, 1-2 March, 2018, Berlin*, 2018.

[5] S. Oertwig, H. Siller, and S. Funke. Advancements in the source localization method SODIX and application to short cowl engine data. In *25th AIAA/CEAS Aeroacoustics Conference, 20-23 May 2019, Delft, The Netherlands*, 2019. AIAA 2019-2743.

[6] Sebastian Oertwig, Timo Schumacher, Henri A. Siller, and Stefan Funke. Extension of the source localization method sodix for coherent sound sources. In *27th AIAA/CEAS Aeroacoustics Conference, 2-6 August 2021, Virtual Event*, 2021.

[7] S. Funke, R. P. Dougherty, and U. Michel. SODIX in comparison with various deconvolution methods. In *5th Berlin Beamforming Conference*, number BeBeC 2014-11, 2014.

[8] D. Blacodon and G. Élias. Level estimation of extended acoustic sources using an array of microphones. In *9th AIAA/CEAS Aeroacoustics Conference and Exhibit, 12-14 May 2003, Hilton Head, South Carolina*, number AIAA 2003-3199, 2003.

[9] D. Blacodon and G. Élias. Level estimation of extended acoustic sources using a parametric method. *Journal of Aircraft*, 41:1360–1369, 2004.

[10] Maximilian Behn, Benjamin Pardowitz, and Ulf Tapken. Compressed sensing based radial mode analysis of the broadband sound field in a low-speed fan test rig. In *Proceedings on CD of the 7th Berlin Beamforming Conference, March 5-6, 2018*. GFaI, Gesellschaft zu Förderung angewandter Informatik e.V., Berlin, March 2018.

[11] Timo Schumacher. Erweiterung eines Ersatzschallquellenverfahrens zur Untersuchung der Schallabstrahlung von Flugzeugtriebwerken auf kohärente Schallquellen. Master's thesis, Technische Universität Berlin, 2020.

[12] E. Sarradj and G. Herold. Acoular - Open-Source-Software zur Anwendung von Mikrofonarrayverfahren. In *DAGA, 42. Jahrestagung für Akustik, 14-17 March, 2016, Aachen*, 2016.